Development of Exact Analytical Solution for Nonlinear Heat transfer Equation of Natural Convection Porous Fin

M. G. Sobamowo[1] and O. A. Adeleye[2]
Department of Mechanical Engineering, University of Lagos, Lagos, Nigeria
Department of System Engineering, University of Lagos, Lagos, Nigeria
Email: msobamowo@unilag.edu.ng

Abstract
The inclusion of nonlinear term in heat transfer models makes it very difficult to develop exact analytical solutions to the problem. Consequently, recourse has been made to numerical or approximate analytical methods. However, the classical way for finding exact analytical solution is obviously still very important since it serves as an accurate benchmark for numerical and approximate analytical solutions. Therefore, in this work, exact analytical solution is developed using Gauss' hypergeometric function for the nonlinear equation arising during heat transfer in porous fin. The developed model was validated with numerical method of solutions and the results were in good agreement. The developed exact analytical model can be compared with other approximate analytical methods found in the literature which are used for solving similar problems

Keywords: *Model, numerical solution, thermal energy.*

1.0 INTRODUCTION

The quests for enhancement and augmentation of the rate of heat dissipation from thermal equipment have made the application of porous fins very necessary and this has led to number of various studies (Ha *et al*., 2005; Kiwan and Al-Nimr, 2001; Kiwan, 2007; Gorla and Bakier, 2008; Bhanja and Kundu, 2011; Taklifi *et al*., 2010; Abbasbandy *et al*., 2011; Saedodin and Sadeghi, 2013; Hatami *et al*., 2013, 2014; Darvishi *et al*., 2015; and Sobamowo, 2016). The nonlinear heat transfer equations that evolve during the thermal modeling of porous fin made it very difficult to generate the exact analytical equation. Consequently, different approximate analytical methods such as Adomian decomposition method (ADM), spectral collocation method (SCM), Homotopy perturbation method (HPM), Homotopy analysis method (HAM), least square method (LSM), variational iterative method (VIM), differential transformation method (DTM) etc. have been applied to provide approximate analytical solutions to the problem (Kundu and Bhanja, 2011; Kundu *et al*., 2012; Taklifi *et al*., 2010; Saedodin *et al*., 2011; Hatami *et al*., 2013, 2014; Darvishi *et al*., 2015, Gorla, *et al*., 2013; Saedodin and Shahbabaei, 2013; Moradi, *et al*., 2014; Hoshyar *et al*., 2015; Rostamiyan *et al*., 2014; and Ghasemi *et al*., 2014). However, the applications of the approximate analytical methods to the nonlinear equations present explicit approximate analytical solutions which often involved mathematical expressions leading to analysis involving large number of terms. In practice, results from such analysis with large number of terms and conditional statements for the solutions are too complex for use by engineers. Consequently, in some other research, recourse has been made to numerical methods in solving the nonlinear problems (Kiwan and Al-Nimr, 2001; Kiwan, 2007; Kiwan and Zeitoun, 2008). However, the classical way of finding exact analytical solution is obviously still very important since it serves as an accurate benchmark for numerical solutions. Exact analytical expressions are required to show the direct relationship between the models parameters. When such exact analytical solutions are available, they provide good insights into the significance of various system parameters affecting the phenomena as it gives continuous physical insights than pure numerical or computation methods. Therefore, in this study, exact analytical solutions are developed for the nonlinear heat transfer equation in porous fin subjected to magnetic field with temperature-dependent internal heat generation. It is hope that the developed exact analytical model will be useful in comparison with other approximate analytical methods found in the literature for similar problems.

2.0 METHODOLOGY

2.1 Theoretical Framework

Consider a porous fin of rectangular profile with temperature-dependent of length L, thickness δ and thermal conductivity *K,* that is exposed on both faces to an environment of convective heat flow and moist air at temperature T_∞ and with heat transfer co-efficient *h* shown in **Figure 1**. In developing the heat transfer model, the following assumptions were made. Porous medium is homogeneous, isotropic and saturated with a single phase fluid

1. Physical properties of solid, as well as fluid are considered as constant except density variation of liquid, which may affect the buoyancy term where Boussinesq approximation is employed.
2. Fluid and porous mediums are locally in thermodynamic equilibrium in the domain.
3. Surface convection, radiative transfers, and non-Darcian effects are negligible and only natural convection is considered. Heat is transferred away from the fin base only through the pores i.e. no convective heat transfer to the surrounding.
4. The temperature variation inside the fin is one-dimensional i.e. temperature varies along the length only and remain constant with time.
5. There is no thermal contact resistance at the fin base and the fin tip is an adiabatic type.

Following the model assumptions, the thermal energy balance could be expressed as in Eq. 1

$$q_x - \left(q_x + \frac{\delta q}{\delta x} dx \right) = \dot{m} c_p (T - T_a) \tag{1}$$

The mass flow rate of the fluid passing through the porous material can be written as in Eq. 2

$$\dot{m} = \rho u(x) W dx \tag{2}$$

From the Darcy's Model (1856), Eq. 3 is derived

$$u(x) = \frac{gK\beta}{v}\left(T - T_a\right) \tag{3}$$

Therefore, Eq. 1 becomes Eq. 4

$$q_x - \left(q_x + \frac{\delta q}{\delta x} dx \right) = \frac{\rho c_p g K\beta}{v} (T - T_a)^2 dx \tag{4}$$

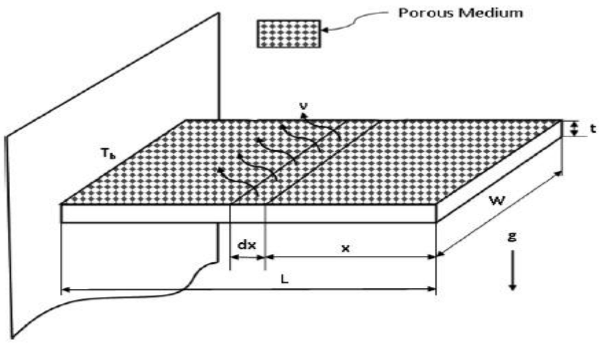

Figure 1: Schematic of the longitudinal natural convection porous fin

As $dx \to 0$, Eq. 4 reduces to Eq. 5

$$-\frac{\delta q}{\delta x} = \frac{\rho c_p g K \beta}{v}(T - T_a)^2 \quad (5)$$

From Fourier's law of heat conduction, Eq. 6 is expressed as:

$$q = -k_{eff} A_{cr} \frac{dT}{dx} \quad (6)$$

Substituting Eq. 6 into Eq. 5, we have Eq. 7

$$\frac{d}{dx}\left(k_{eff} A_{cr} \frac{dT}{dx}\right) = \frac{\rho c_p g K \beta}{v}(T - T_a)^2 \quad (7)$$

Further simplification of Eq. 7 gives the governing differential equation for the fin as in Eq. 8

$$\frac{d^2 T}{dx^2} - \frac{\rho c_p g K \beta}{t v k_{eff}}(T - T_a)^2 = 0 \quad (8)$$

where $k_{eff} = \phi k_f + (1 - \phi) k_s$

The boundary conditions are expressed in Eq. 9

$$x = 0, \quad \frac{dT}{dx} = 0$$
$$x = L, \quad T = T_b \quad (9)$$

The following dimensionless parameters in Eq. 9 were substituted into Eq. 8 to give Eq. 10;

$$X = \frac{x}{L}, \quad \theta = \frac{T - T_\infty}{T_b - T_\infty}, \; Ra = Gr.\Pr = \left(\frac{\beta' g T_b t^3}{\nu_f^2}\right)\left(\frac{\rho c_p \nu_f}{k_{eff}}\right),$$
$$Da = \frac{K}{t^2}, \quad (10)$$

$$S_h = \left(\frac{\beta' g (T_b - T_\infty) t^3}{\nu_f^2}\right)\left(\frac{\rho c_p \nu_f K}{k_{eff} t^2}\right)\frac{(L/t)^2}{k_{eff}} = \frac{Ra Da (L/t)^2}{k_{eff}}$$

The dimensionless governing differential is Eq. 11 and the boundary conditions, is Eq. 12.

$$\frac{d^2\theta}{dX^2} - S_h\theta^2 = 0 \tag{11}$$

The boundary conditions are

$$X = 0, \quad \frac{d\theta}{dX} = 0$$
$$X = 1, \quad \theta = 1 \tag{12}$$

2.2 Development of exact analytical solutions

Although, the nonlinear Eq. 11 looks somehow simple, it has been very difficult to develop an exact analytical/closed-form solution for the equation. However, in this work, an attempt was made to provide an exact analytical solution through the use of special function. The procedures for obtaining the exact solution are given as follows.

In order to find exact analytical solution for Eq. 11, taking the transformation $\frac{d\theta}{dX} = \phi$, we arrived at Eq. 13

$$\phi\frac{d\phi}{dX} - S_h\theta^2 = 0 \tag{13}$$

On integrating Eq. 13 w.r.t θ, we have Eq. 14

$$\frac{\phi^2}{2} - \frac{S_h}{3}\theta^3 = C \tag{14}$$

Recall that $\phi = \frac{d\theta}{dX} \quad \rightarrow \phi^2 = \left(\frac{d\theta}{dX}\right)^2$

Therefore, Eq. 14 becomes Eq. 15

$$\frac{1}{2}\left(\frac{d\theta}{dX}\right)^2 - \frac{S_h}{3}\theta^3 = C \tag{15}$$

With the application of the first boundary condition, $X = 0, \quad \frac{d\theta}{dX} = 0 \quad \rightarrow X = 0, \quad \theta = \theta_o$

$$C = -\frac{S_h}{3}\theta_o^3 \tag{16}$$

On substituting Eq. 16 into Eq. 15, we arrived at Eq. 17

$$\frac{1}{2}\left(\frac{d\theta}{dX}\right)^2 - \frac{S_h}{3}\left(\theta^3 - \theta_o^3\right) = 0 \tag{17}$$

which could be written as in Eq. 18

$$\left(\frac{d\theta}{dX}\right)^2 - \frac{2S_h}{3}\theta^3 + \frac{2S_h}{3}\theta_o^3 = 0 \tag{18}$$

Then

$$dX = \frac{d\theta}{\sqrt{\frac{2S_h}{3}\theta^3 - \frac{2S_h}{3}\theta_o^3}} \tag{19}$$

Since θ increases as x increases, the positive sign is used when taking the square root . Integrating Eq. 19 as in Eq. 20.

$$\int_0^X dX = \sqrt{\frac{3}{2S_h}}\int_{\theta_o}^{\theta}\frac{d\theta}{\sqrt{\theta^3 - \theta_o^3}} \tag{20}$$

which gives Eqs. 21 and 22.

$$X = \frac{1}{\sqrt{2}}\left[\frac{-\theta_o\left(\sqrt{\pi}\,\Gamma\left(\frac{1}{6}\right) + 2\left(\frac{\theta_o}{\theta}\right)^{\frac{1}{2}}\Gamma\left(\frac{-1}{3}\right)F_1\right)}{\sqrt{\left(\frac{\theta_o^3 S_h}{3}\right)}\,\Gamma\left(\frac{-1}{3}\right)}\right] \tag{21}$$

$where$

$$F_1 = F\left(\frac{1}{2},\frac{1}{6},\frac{3}{2}-\frac{1}{3},\left(\frac{\theta_o}{\theta}\right)^3\right)$$

or

$$X = \sqrt{\frac{2}{3S_h\theta_o}}\left[\left(\frac{\theta}{\theta_o}\right)^{-2}\sqrt{\left[\left(\frac{\theta}{\theta_o}\right)^3 - 1\right]}F_2\right]$$

$where$

$$F_2 = F\left(1,\frac{1}{2},\frac{3}{2},1-\left(\frac{\theta}{\theta_o}\right)^{-3}\right) \tag{22}$$

Where θ_o is an unknown dimensionless tip temperature and the generalized hypergeometric functions is given as in Eq. 23.

$${}_pF_q\left(\alpha_1,\alpha_2,...,\alpha_p;\gamma_1,\gamma_2,...,\gamma_q;z\right) = \sum_{k=0}^{\infty}\frac{\prod_{i=1}^{p}\left(\alpha_i\right)_k z^k}{\prod_{j=1}^{q}\left(\gamma_j\right)_k k!} \tag{23}$$

Then, Eq. 24 can be expressed as:

$$\begin{aligned}{}_2F_1\left(a,b,c,z\right) &= \sum_{k=0}^{\infty}\frac{(a)_k(b)_k z^k}{(c)_k k!}\\ &= \frac{\Gamma(c)}{\Gamma(a)\Gamma(b)}\sum_{k=0}^{\infty}\frac{\Gamma(a+k)\Gamma(b+k)}{\Gamma(c+k)}\frac{z^k}{k!}\end{aligned} \tag{24}$$

The Gauss's hypergeometric function $F\left(a,b,c,z\right)$ is given as in Eqs. 25 to 27.

$$F(a,b,c,z) = Gauss'\ hypergeometric\ \ function\ {}_2F_1(a,b,c,z) = \frac{\Gamma(c)}{\Gamma(c)\Gamma(c-b)}\int_0^1 t^{a-1}(1-t)^{c-a-1}(1-tz)^{-b}\,dt \tag{25}$$

Therefore,

$$F\left(\frac{1}{2},\frac{1}{6},\frac{7}{6},\left(\frac{\theta_o}{\theta}\right)^3\right) = \sum_{k=0}^{\infty}\frac{\left(\frac{1}{2}\right)_k\left(\frac{1}{6}\right)_k\left(\frac{\theta_o}{\theta}\right)^{3k}}{\left(\frac{7}{6}\right)_k k!}$$

$$= \frac{\Gamma\left(\frac{7}{6}\right)}{\Gamma\left(\frac{1}{2}\right)\Gamma\left(\frac{1}{6}\right)}\sum_{k=0}^{\infty}\frac{\Gamma\left(\frac{1}{2}+k\right)\Gamma\left(\frac{1}{6}+k\right)}{\Gamma\left(\frac{7}{6}+k\right)}\frac{\left(\frac{\theta_o}{\theta}\right)^{3k}}{k!} \tag{26}$$

$$x = \frac{1}{\sqrt{2}}\left[\frac{-\theta_o\left(\sqrt{\pi}\,\Gamma\left(\frac{1}{6}\right)+2\left(\frac{\theta_o}{\theta}\right)^{\frac{1}{2}}\Gamma\left(\frac{-1}{3}\right)\frac{\Gamma\left(\frac{7}{6}\right)}{\Gamma\left(\frac{1}{2}\right)\Gamma\left(\frac{1}{6}\right)}\sum_{k=0}^{\infty}\frac{\Gamma\left(\frac{1}{2}+k\right)\Gamma\left(\frac{1}{6}+k\right)}{\Gamma\left(\frac{7}{6}+k\right)}\frac{\left(\frac{\theta_o}{\theta}\right)^{3k}}{k!}\right)}{\sqrt{\frac{\theta_o^3 S_h}{3}}\,\Gamma\left(\frac{-1}{3}\right)}\right] \tag{27}$$

The unknown θ_o in the solution was determined by using the second boundary condition; thus Eq. 27 gives the value for the unknown θ_o.

3.0 RESULTS AND DISCUSSION

The exact analytical method of solution for the non-linear thermal model was validated by the fourth-Order Runge Kutta with shooting algorithm as presented by Kiwan (2007b) and also with the numerical method (NM) and homotopy perturbation method (HPM) results as presented by Petroudi *et al.* (2012) as shown in **Figures 2-4**.

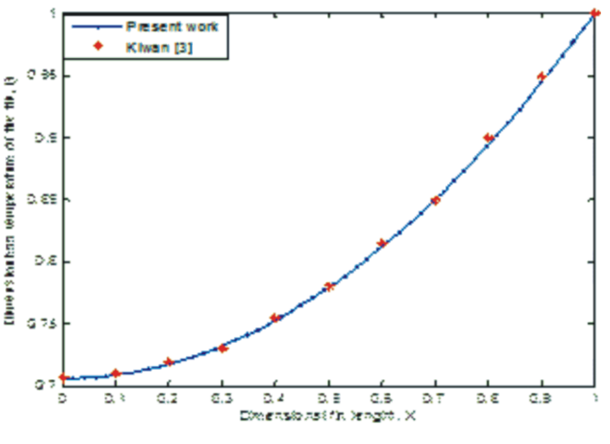

Figure 2: Comparison of results for S_h=1

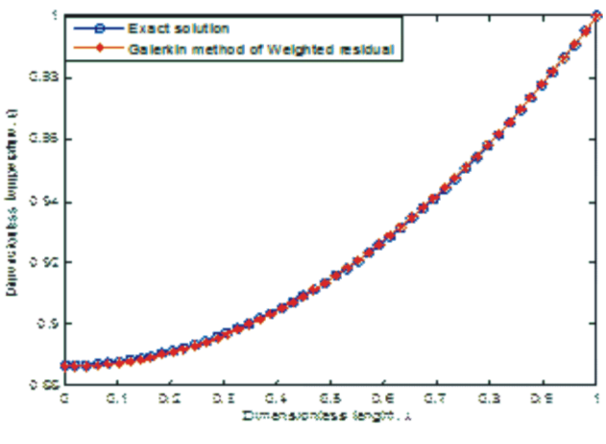

Figure 3: Comparison of GMWR and Exact results

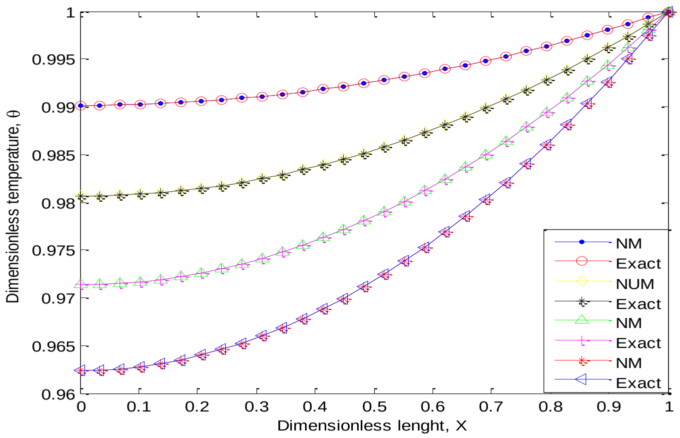

Figure 4: Comparison of GMWR and Exact results

Figure 4 shows the effects of porous parameter on the temperature distribution in the fin. From the results, it was observed that as the porosity parameter increases, the temperature decreases rapidly. An increase in the rate of heat transfer through the fin was also observed as the temperature in the fin drops (this becomes steeper i.e. reflecting high base heat flow rates) as shown in the **Figures 2 – 4**. The rapid decrease in fin temperature due to increase in the porosity parameter is because as porosity parameter, Raleigh number increases, the permeability of the porous fin increases and therefore the ability of the working fluid to penetrate through the fin pores increases. The effect of buoyancy force increases and thus the fin transfer more heat, the rate of heat dissipation or transfer from the fin is enhanced and there is an increase in the thermal performance of the fin. Therefore, increase in the porosity of the fin improves fin efficiency due to increasing in convection heat transfer.

It is hope that the developed exact analytical model will serve as basis for comparison of any other method of analysis of the problem as displayed in this paper. **Table 1** shows comparison of results. From the results, we could establish that good agreements are reached between the present exact analytical solutions and the numerical solutions.

Table 1: Comparison of result

X	NM	GMWR	Exact solution (The Present study)
0.00	0.9581	0.9581	0.9582
0.10	0.9585	0.9585	0.9584
0.20	0.9597	0.9597	0.9595
0.30	0.9618	0.9618	0.9620
0.40	0.9647	0.9647	0.9648
0.50	0.9685	0.9685	0.9684
0.60	0.9730	0.9731	0.9730
0.70	0.9785	0.9785	0.9785
0.80	0.9846	0.9847	0.9848
0.90	0.9919	0.9919	0.9918
1.00	1.0000	1.0000	1.0000

4.0 CONCLUSION

Exact analytical solutions for the nonlinear equation arising during heat transfer in porous fin has been studied. The developed model has been validated with numerical method of solutions and the results were in good agreement. The developed exact analytical model can be compared with other approximate analytical methods found in the literature which are used for solving similar problems. The model also provide platform for the exact analysis and improvement in the design of porous fin in heat transfer equipment.

REFERENCES

Abbasbandy, S., Shivanian, E. and Hashim, I. (2011). Exact analytical solution of a forced convection in porous-saturated duct, *Communication Nonlinear Science Numerical Simulation*, 16, 3981–3989.

Bhanja, D. and Kundu, B. (2011). Thermal analysis of a constructal T-shaped porous fin with radiation effects, *International Journal of Refrigeration* 34, 1483–96.

Darvishi, M. T., Gorla, R., Khani, R.S. and Aziz, F., A.-E. (2015). Thermal performance of a porous radial fin with natural convection and radiative heat losses, *Thermal Science*, 19**(2):** 669-678.

Ghasemi, S. E., Valipour, P., Hatami, M. and Ganji, D. D. (2014). Heat transfer study on solid and porous convective fins with temperature-dependent heat -generation using efficient analytical method, *Journal of Central South University*, 21, 4592−4598.

Gorla, R. S. and Bakier, A. Y. (2011). Thermal analysis of natural convection and radiation in porous fins, *International Communication on Heat Mass Transfer* 38, 638-645.

Gorla, R., Darvishi, R. S. and Khani, M. T., (2013). Effects of variable Thermal conductivity on natural convection and radiation in porous fins. *International Communication on Heat Mass Transfer* 38, 638-645.

Ha, H., Ganji, D. D and Abbasi, M. (2015). Determination of Temperature Distribution for Porous Fin with Temperature-Dependent Heat Generation by Homotopy Analysis Method, *Journal of Applied Mechanics in Engineering*, 4**(1):** 1-5.

Hatami, M., Ahangar, G. H. R. M. and Ganji, D. D., (2014). Boubaker K., Refrigeration efficiency analysis for fully wet semi-spherical porous fins. *Energy Conversion and Management*, 84, 533−540.

Hatami, M. and Ganji, D. D., (2013). Thermal performance of circular convective-radiative porous fins with different section shapes and materials. *Energy Conversion and Management*, 76, 185−193.

Hatami, M. and Ganji, D. D., (2014). Investigation of refrigeration efficiency for fully wet circular porous fins with variable sections by combined heat and mass transfer analysis. *International Journal of Refrigeration*, 40, 140−151.

Hatami, M. and Ganji, D. D., (2014). Thermal behavior of longitudinal convective–radiative porous fins with different section shapes and ceramic materials (SiC and Si3N4), *International Journal of Ceramics*, 40, 6765−6775.

Hatami, M., Hasanpour, A. and Ganji, D. D., (2013). Heat transfer study through porous fins (Si3N4 and AL) with temperature-dependent heat generation, *Energy Conversion and Management*, 74, 9-16.

Hoshyar, H. A., Rahimipetroudi, I., Ganji, D. D. and Majidian, A. R., (2015). Thermal performance of porous fins with temperature-dependent heat generation via Homotopy perturbation method and collocation method, *Journal of Applied Mathematics and Computational Mechanics*, 14**(4**): 53-65.

Kiwan, S. (2007). Thermal analysis of natural convection porous fins, *Transport Porous Media* 67, 17-29.

Kiwan, S., (2007). Effect of radiative losses on the heat transfer from porous fins, *International Journal of Thermal Science*, 46, 1046-1055

Kiwan, S. and Al-Nimr, A., (2001). Using Porous Fins for Heat Transfer Enhancement, *ASME Journal of Heat Transfer*, 123: 790–5.

Kiwan, S. and Zeitoun, O., (2008). Natural convection in a horizontal cylindrical annulus using porous fins, *International* Journal of Numerical Heat Fluid Flow 18 **(5):** 618-634.

Kundu, B., Bhanja, D. and Lee, K. S. (2012). A model on the basis of analytics for computing maximum heat transfer in porous fins, *International Journal of Heat Mass Transfer* 55 **(25-26):** 7611-7622.

Kundu, B. and Bhanja, D. (2011). An analytical prediction for performance and optimum design analysis of porous fins, *International Journal of Refrigeration* 34, 337-352.

Moradi, A., Hayat, T. and Alsaedi, A., (2014). Convective-radiative thermal analysis of triangular fins with temperature-dependent thermal conductivity by DTM, *Energy Conversion and Management* 77, 70–77

Petroudi, I. R, Ganji, D. D., Shotorban, A. B., Nejad, M. K., Rahimi, E., Rohollahtabar, R. and Taherinia, F. (2012). Semi-Analytical Method for Solving Nonlinear Equation Arising in Natural Convection Porous fin, *Thermal Science*, 16**(5):** 1303-1308.

Rostamiyan, Y., Ganji, D. D., Petroudi, I. R., and Nejad, M. K., (2014). Analytical Investigation of Nonlinear Model Arising in Heat Transfer Through the Porous Fin, *Thermal Science*, 18**(2**): 409-417.

Saedodin, S. and Olank, M., (2011). Temperature Distribution in Porous Fins in Natural Convection Condition, *Journal of American Science* 7**(6):** 476-481.

Saedodin, S. and Sadeghi, S., (2013). Temperature distribution in long porous fins in natural convection condition, *Middle-east Journal of Science Res*. 13 **(6):** 812-817.

Saedodin, S. and Shahbabaei, M. (2013). Thermal Analysis of Natural Convection in Porous Fins with Homotopy Perturbation Method (HPM), *Arab Journal of Science Engineering* 38:2227–2231.

Sobamowo, M. G. (2016). Thermal analysis of longitudinal fin with temperature-dependent properties and internal heat generation using Galerkin's method of weighted residual, *Applied Thermal Engineering* 99, 1316–1330.

Taklifi, A., Aghanajafi, C. and Akrami, H., (2010). The effect of MHD on a porous fin attached to a vertical isothermal surface, *Transport Porous Media*, 85, 215–31.

Nomenclature

A_c cross sectional area of the fins
A_p profile area of the fins
Bi Biot number
c_p specific heat capacity, kJ/(kg /C)
Da Darcy number
Gr Grashof number
K thermal conductivity of the fin material
k_a thermal conductivity of the fin material at ambient temperature
k_b thermal conductivity of the fin material at the base temperature of the fin
L Length of the fin
M dimensionless thermo-geometric fin parameter
m thermo-geometric fin parameter
P perimeter of the fin
Pr Prandtl number
Ra Rayleigh number
S_h porosity number
t thickness of the fin
T Temperature
T_∞ ambient temperature
T_b Temperature at the base of the fin
x fin axial distance, m
X dimensionless length of the fin
u, V velocity
δ fin base thickness

Greek Symbols

σ conductivity of the medium
θ dimensionless temperature
θ_b dimensionless temperature at the base of the fin
ρ density of the fin